Geometric optimization of micro-thermoacoustic cooler for heat management in electronics

K.Tartibu, B.Sun and M.A.E. Kaunda
Department of Mechanical Engineering
Cape Peninsula University of Technology Box 652
Cape Town 8000, South Africa
Email: tartibuk@cput.ac.za

***Abstract*—As a result of miniaturisation, electronic products are shrinking in size and weight but with greater pressure for cost reduction. Heat fluxes have increased considerably and hence thermal management becomes crucial from the reliability point of view. Thermoacoustic heat engines provide a practical solution to the problem of heat management in microcircuits where they can be used to pump heat or produce spot cooling of specific circuit elements. However, the most inhibiting characteristic of thermoacoustic cooling is its current lack of efficiency. A multiobjective optimization approach is presented to model and optimize a small-scale thermoacoustic regenerator. Optimization of multiple objectives components is considered and global optimal solutions have been identified using the epsilon constraint method.**

I. INTRODUCTION

Thermal management has always been a concern for computer systems and other electronics. Computational speeds will always be limited by the amount of noise produced by computer chips. Since most noise is generated by wasted heat, computer components and other semiconductor devices operate faster and more efficiently at lower temperatures [1]. The need to manage heat fluxes of order 10–50 W/cm^2 and higher in microcircuits has emphasized the importance of developing devices which can cope with such heat levels. Many interesting devices have been proposed for such applications. They range from forced convection cooling devices to thermoelectric devices, heat pipes, liquid coolants, and evaporative spray cooling devices [2].

Here thermoacoustic devices are proposed (Fig. 1); such engines can convert heat to sound or use sound to pump heat. They are a new application in the area of thermal management but based on their performance and adaptability to microcircuits they show much promise [3]. If thermoacoustic cooling devices could be scaled for computer applications, the electronic industry would realize longer lifetimes for microchips, increased speed and capacity for telecommunications, as well as reduced energy costs [4].

The basic mechanics behind thermoacoustics are already well understood. A detailed explanation of the way thermoacoustic coolers work is given by Swift [5] and Wheatly et al. [6]. Research is focusing on optimizing the method so that thermoacoustic coolers can compete with commercial refrigerators. The presence of a stack provides heat exchange with the sound field and the generation or absorption of acoustic power. With a suitable geometry substantial amounts of heat can be moved as demonstrated, for example, by Garrett and Hofler [7]. An interesting and important feature of such engines is that the performance depends on geometric factors and gas parameters [8].

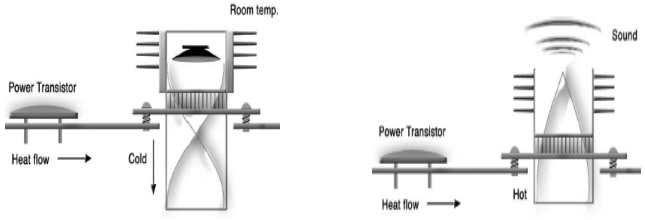

Fig. 1. (a) Acoustic spot-cooler interfaced with circuit (b) Prime mover interfaced with circuit [3]

Optimization techniques as a design supplement are severely under-utilized, and previous efforts in the optimization of thermoacoustic devices are rare. Minner et al. [9], Wetzel [10], Besnoin [11] and Tijani et al. [12] utilized a linear approach while trying to optimize the device. Additionally, most studies (the exception being the Minner et al. study) vary only a single parameter, holding all else fixed and ignored thermal losses to the surroundings. These Parametric studies are unable to capture the nonlinear interactions inherent in thermoacoustic models with multiple variables, and can only guarantee locally optimal solutions.

Zink et al [13] and Trapp et al. [14] illustrate the optimization of thermoacoustic systems, while taking into account thermal losses to the surroundings that are typically disregarded. They use mathematical analysis and optimization and illustrate the conflicting nature of objective component considered in their modeling approach. In spite of their introductory nature, the presented works are important contributions to thermoacoustics as it merges the theoretical optimization approach with thermal investigation in thermoacoustics. Therefore since several conflicting objectives have been identified, an effort to effectively implement the epsilon constraint method for producing the Pareto optimal solutions in a multiobjective optimization mathematical programming method is carried out in our approach. This has been implemented in the widely used modeling language

GAMS [15] (General Algebraic Modeling Language, www.gams.com). As a result, Gams codes are written to define, to analyze, and solve optimization problems to generate sets of Pareto optimal solutions unlike previous studies.

The remainder of this paper is organized in the following fashion: the fundamental components of our mathematical model characterizing the standing wave thermoacoustic heat engine are presented in Section 2. Section 3 illustrates our optimization procedure. Section 4 considers multiobjective optimization using epsilon constraint method. In Section 4, we conclude by suggesting possible future extension of this work.

II. Modelling Approach

In this section, our modelling approach for the physical standing wave engine depicted in Fig. 2 is discussed; the development of our mathematical model and its corresponding optimization is included. The problem is reduced to a two dimensional domain, because of the symmetry present in the stack. Two constant temperature boundaries are considered namely one convective boundary and one adiabatic boundary, as shown in Fig. 2. For our model, only the regenerator geometry is considered; the model considers variation in operating condition and the interdependency of stack location and geometry.

Five different parameters are considered to characterize the regenerator:

- L: Stack length,
- H: stack height,
- Za: stack placement (with Za=0 corresponding to the closed end of the resonator tube),
- d: channel diameter, and
- N: number of channels.

Those parameters have been allowed to vary simultaneously. Five different objectives as described by Trapp et al. [14] namely two acoustic objectives (Acoustic work W of the thermoacoustic engine and viscous resistance R_V through the regenerator [16]) and three thermal objectives (convective heat flow Q_{conv}, radiative heat flow Q_{rad}, and conductive heat flow Q_{cond}) are considered to measure the quality of a given set of variable value that satisfies all of the constraint. Because work is the only objective to be maximized, we instead minimize its negative magnitude along with all of the other components. Ultimately, optimizing the resulting problem generates optimal objective function value $G^* = \left[W^*, R_V^*, Q_{conv}^*, Q_{rad}^*, Q_{cond}^*\right]$ and optimal solution $x^* = \left[L^*, H^*, d^*, Za^*, N^*\right]$.

Since the five objectives are conflicting in nature [14], a multiobjective optimization approach has been used. Those objectives are conflicting in the sense that, if optimized individually, they do not share the same optimal solutions. Since we optimize multiple objective components simultaneously, each objective component has been given a weighting factor w_i to provide appropriate user-defined emphasis.

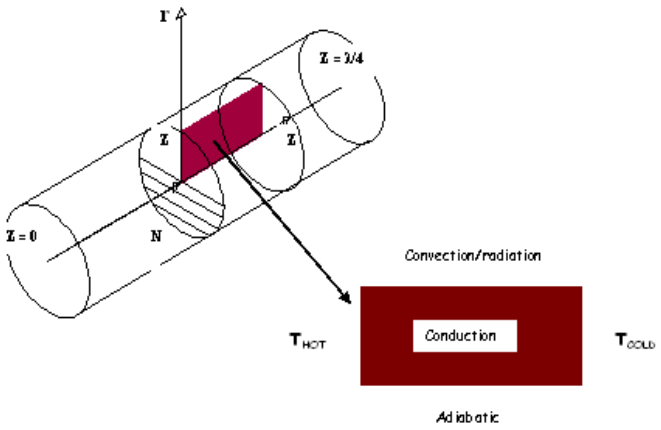

Fig.2. Computational domain

According to Hwang and Masud [17], the methods for solving multiobjective mathematical programming problems can be classified into three categories, based on the phase in which the decision maker involves in the decision making process expressing his/her preferences: the a priori methods, the interactive methods and the a posteriori or generation methods. The a posteriori (or generation) methods give the whole picture (i.e. the Pareto set) to the decision maker, before his/her final choice, reinforcing thus, his/her confidence to the final decision. In general, the most widely used generation methods are the weighting method and the ε-constraint method. These methods can provide a representative subset of the Pareto set which in most cases is adequate. The basic step towards further penetration of the generation methods in our multiobjective mathematical problems is to provide appropriate codes in a Gams environment and produce efficient solutions.

III. Illustration of the Optimization Procedure of the Regenerator

The five variables L, H, d, Za, N may only take values within the certain lower and upper bounds. The feasible domain for a thermoacoustic regenerator is defined as follow:

$$\begin{aligned} L_{min} \le L \le L_{max} \\ H_{min} \le H \le H_{max} \\ d_{min} \le d \le d_{max} \\ Za_{min} \le Za \le Za_{max} - L \\ N_{min} \le N \le N_{max} \end{aligned} \qquad (1)$$

$L,\ H,\ d,\ Za \in \Re+$ and $N \in Z+$

Additionally, the total number of channels N of a given diameter d is limited by the cross-sectional radius of the resonance tube H. Therefore the following constraint relation can be determined:

$$N(d + t_w) \le 2H \qquad (2)$$

where t_w represents the wall thickness around a single

channel. The relation between the stack perimeter $\prod$ and the cross sectional area A as determined by Swift [16] is given by:

$$\prod = \frac{2A}{d + tw} \tag{3}$$

The following boundary conditions must also be enforced:

1. Constant hot side temperature (T_h),

2. Constant cold side temperature (T_C),

3. Adiabatic boundary, modeling the central axis of the cylindrical stack:

$$\left.\frac{\partial T}{\partial r}\right|_{r=0} = 0; \tag{4}$$

4. Free convection and radiation to surroundings (at T_∞) with temperature dependent heat transfer coefficient (h), emissivity ε, and thermal conductivity (k):

$$k\left.\frac{\partial T}{\partial r}\right|_{r=H} = h(T_S - T_\infty) + \varepsilon k_b\left(T_S^4 - T_\infty^4\right) \tag{5}$$

The acoustic power per channel has been derived by Swift [15]. The following equation can be derived for N channel:

$$W = \omega LN\left(\frac{\pi H^2}{2(d + t_w)}\right)\left[\delta_k \frac{(\gamma - 1)p^2}{\rho c^2 (1 + \varepsilon)}(\nabla T_{crit.} - 1) - \delta_v \rho u^2\right] \tag{6}$$

The thermal penetration depth δ_k, the viscous penetration depth δ_v and the critical temperature are given by the following equations:

$$\delta_k = \sqrt{\frac{2K}{\rho_m c_p \omega}} \tag{7}$$

$$\delta_V = \sqrt{\frac{2\mu}{\rho_m \omega}} \tag{8}$$

$$\nabla T_{crit.} = \frac{\omega p_1^s}{\rho_m c_p u_1^s} \tag{9}$$

With K being the thermal conductivity, ρ_m the mean density, c_p the constant pressure specific heat, μ is the diffusivity of the working fluid and ω the operating frequency.

The amplitudes of the dynamic pressure p and gas velocity u due to the standing wave in the tube are given by:

$$p = p_{max}\cos\left(\frac{2\pi Za}{\lambda}\right) \tag{10}$$

$$u = u_{max}\sin\left(\frac{2\pi Za}{\lambda}\right) \tag{11}$$

$$\text{with } u_{max} = \frac{p_{max}}{\rho.c} \tag{12}$$

The heat capacity ratio can be expressed by [16]:

$$\varepsilon = \frac{(\rho c_p \delta_k)_g}{(\rho c_p \delta_s)_s}\frac{\tanh((i+1)y_0/\delta_k)}{\tanh((i+1)l/\delta_s)} \tag{13}$$

This expression can be simplified to values of $\varepsilon = y_0/\delta_k$ if $y_0/\delta_k < 1$ and $\varepsilon = 1$ if $y_0/\delta_k > 1$ [13], where y_0 half of the channel height is, l is half of the wall thickness and δ_s is the solid's thermal penetration depth.

Just as the total acoustic power of the stack was dependent on the total number of channels, the viscous resistance also depends on his value. The following equation can be derived:

$$R_V = \frac{\mu \prod L}{A_C^2 \delta_V N} = \frac{2\mu}{\delta_V}\frac{L}{(d + t_w)\pi H^2 N} \tag{14}$$

The heat transfer coefficient and the heat flux to the surroundings were estimated using a linear temperature profile. In this model, the actual temperature distribution throughout the stack is taken into account by utilizing MATLAB finite element toolbox [18], which captures the temperature dependence of the heat transfer coefficient. Only the temperature distribution at the shell surface and the temperature gradient at the cold side are of interest. Trapp et al. [13] have derived the final surface temperature distribution as a function of axial direction Za. It is given by:

$$T_S = T_h e^{\ln\left(\frac{T_C}{T_h}\right)\frac{Za}{L}} \tag{15}$$

The convective heat transfer coefficient and the radiative heat flux to the surroundings are assumed to be dependent on the temperature. The total convective heat transfer across the cylindrical shell in its integral form can be described by:

$$Q_{conv} = H\int_0^{2\pi L}\int_0 h(T(x))(T(x) - T_\infty)dxd\rho \tag{16}$$

It is shown for the case of a horizontal tube subject to free convection [18], the heat transfer coefficient h is derived from the Nusselt number, which is a non-dimensional heat transfer coefficient as follow:

$$h(Ts) = \frac{k_g}{2H}Nu \tag{17}$$

$$Nu = 0.36 + \frac{0.518Ra_D^{\frac{1}{4}}}{\left[1 + \left(\frac{0.559}{Pr}\right)^{\frac{9}{16}}\right]^{\frac{4}{9}}} \tag{18}$$

This expression depends on the Prandtl number, which can be expressed by:

$$Pr = \frac{\nu}{\alpha} \tag{19}$$

$$Ra = \frac{g\beta(T_S - T_\infty)8H^3}{\nu\alpha} \tag{20}$$

where Pr is the Prandtl number, T_S is the surface temperature, T_∞ is the (constant) temperature of the surroundings, ν is the viscosity of the surrounding gas, and α is the thermal diffusivity of the surrounding gas (air). The temperature distribution stated in Eq.15 is then used to determine the convective heat transfer to the surroundings.

After integrating we derive the following heat flow expressions:

$$Q_{conv} = 2\pi HLh\left[\frac{T_C - T_H}{\ln\left(\frac{T_C}{T_H}\right)} - T_\infty\right] \quad (21)$$

The radiation heat flux becomes increasingly important as T_H increases, as shown in the following equation:

$$Q_{rad} = Hk_B \int_0^{2\pi L}\int_0 \varepsilon\left(T(x)^4 - T_\infty^4\right)dxd\rho \quad (22)$$

Where k_B is the Stefan Boltzmann constant, and ε is the surface emissivity, which depends on the emitted wavelength, and in turn is a function of temperature. After integrating we derive the following heat flow expressions:

$$Q_{rad} = 2\pi HLk_B\varepsilon\left[\frac{T_C^4 - T_H^4}{4\ln\left(\frac{T_C}{T_H}\right)} - T_\infty^4\right] \quad (23)$$

The conductive heat flux is representative of the heat loss across the cold end of the domain. As the temperature gradient there is non-zero, a heat flux must be present. It is assumed that thermal energy is removed via the cooling water flow. Similar to the cylindrical shell, this heat flux has to be integrated over the whole surface representing the cold side:

$$Q_{cond} = \int_0^{2\pi}\int_0^H \left(k_{zz}\frac{\partial T}{\partial r}\right)drd\rho \quad (24)$$

Where the value of the axial thermal conductivity k_{zz} is determined by the following equation:

$$k_{zz} = \frac{k_S t_w + k_g d}{t_w + d} \quad (25)$$

The temperature distribution is used to determine the temperature gradient at the top surface Za, $r = H$ .The general statement of Fourier law of thermal conduction expressed as $\frac{\Delta Q}{\Delta t} = -kA\frac{\Delta T}{\Delta x}$ is used to determine the heat flow. Therefore: $\left.\frac{\partial T}{\partial z}\right|_{z=L} = \frac{\ln\left(\frac{T_C}{T_H}\right)\left(\frac{T_C}{T_H}\right)}{L}$ (26)

And $Q_{cond} = \frac{k_{zz}}{L}\pi H^2 T_C \ln\left(\frac{T_H}{T_C}\right)$ (27)

IV. EMPHASIZING ALL OBJECTIVE COMPONENTS

All the expressions involved in our mathematical model (MPF) have been presented in the previous section. Together with the following expressions, they represent a non-linear mixed integer program:

$$(\text{MPF}) \min_{L,H,Z_a,d,N} \xi = w_1(-W) + w_2 R_V + w_3 Q_{conv} + w_4 Q_{rad} + w_5 Q_{cond} \quad (28)$$

There is no single optimal solution that simultaneously optimizes all the two objectives functions. In these cases, the decision makers are looking for the "most preferred" solution. To find the most preferred solution of this multiobjective model, we apply the augmented ε-constraint method (AUGMECON) as proposed by Mavrotas [20]. The ε-constraint method has several important advantages over traditional weighted method. These advantages are listed in [20]. In the conventional ε-constraint method, there is no guarantee that the obtained solutions from the individual optimization of the objective functions are Pareto optima or efficient solutions. In other to overcome this deficiency, the lexicographic optimization for each objective functions to construct the payoff table for the multiobjective mathematical programming (MMP) is proposed here in other to yield just Pareto optimal solutions. The mathematical details of computing payoff table for MMP problem can be found in [21]. The augmented ε-constraint method for solving model (Eq.35) can be shown as follows:

$$\max\left(F_1(x) + eps \times \left(\frac{s_2}{r_2} + \frac{s_3}{r_3} + \ldots + \frac{s_p}{r_p}\right)\right)$$

$$\text{s.t.} \quad F_2(x) - s_2 = e_2$$

$$F_3(x) - s_3 = e_3 \quad (29)$$

$$\ldots$$

$$\max F_p(x) - s_p = e_p$$

$$x \in S \text{ and } s_i \in \Re^+$$

To illustrate our approach, we consider the thermoacoustic couple (TAC) as described in [22]. It consists of a parallel-plate stack placed in helium-filled resonator. All relevant parameters are given in Table I and Table II.

TABLE I: Specifications for Thermoacoustic couple

Parameter	Symbol	Value	Unit
Isentropic coefficient	ν	1.67	
Gas density	ρ	0.16674	kg/m^3
Specific heat capacity	c_p	5193.1	J/kg.K
Dynamic viscosity	μ	$1.9561.10^{-5}$	kg/m.s
Maximum velocity	u_{max}	670	m/s
Maximum pressure	p_{max}	114003	Pa
Speed of sound	c	1020	m/s
Thickness plate	t_w	1.91.10-4	M
Frequency	f	696	Hz
Thermal conductivity Helium	k_g	0.16	W/(m.K)
Thermal conductivity stainless steel	k_S	11.8	W/(m.K)
Isobaric specific heat capacity	c_p	5193.1	J/(kg.K)

TABLE II: Additional parameters used for programming

Parameter	Symbol	Value	Unit
Temperature of the surrounding	T_∞	298	K
Constant cold side temperature	T_C	300	K
Constant hot side temperature	T_H	700	K
Wavelength	λ	1.466	m
Thermal expansion	β	$1/T_\infty$	1/K
Thermal diffusivity	α	2.1117E-5	m2s-1

The following constraints (upper and lower bounds) have been enforced on variables in other for the solver to carry out the search of the optimal solutions in those ranges:

$$\begin{aligned} &L.lo = 0.005; \quad L.up = 0.05; \\ &Za.lo = 0.005; \\ &H.lo = 0.005; \\ &d.lo > 2.\delta_k; \quad d.up < 4.\delta_k \end{aligned} \tag{30}$$

We use lexicographic optimization for the payoff table, the application of model (Eq.29) will provide only the Pareto optimal solutions (like in the previous case), avoiding the weakly Pareto optimal solutions. Efficient solutions of the proposed model have been found using AUGMENCON method and the LINDOGLOBAL solver. To save computational time, the early exit from the loops as proposed by Mavrotas [20] has been applied. The integer variable N has been given values of 20 to 50. This process generates optimal solutions corresponding to each integer variable. The following section report only sets of Pareto solutions obtained:

TABLE III: Non-dominated solutions found by AUGMENCON

N	L^*	d^*	H^*	Za^*	CPU time (s)
26	0.050	0.00091589	0.014	0.005	4151.219
31	0.006	0.00058140	0.012	0.005	11317.03
33	0.006	0.00058140	0.013	0.006	8880.250
36	0.050	0.00108681	0.022	0.005	3288.672
38	0.005	0.00059305	0.015	0.005	7109.984
39	0.008	0.00113555	0.026	0.005	8153.719
40	0.046	0.00112554	0.027	0.005	3073.156
42	0.049	0.00079919	0.021	0.005	3347.157
43	0.050	0.00091167	0.024	0.005	3420.937
45	0.041	0.00110152	0.030	0.005	2838.093
49	0.006	0.00058146	0.019	0.005	10124.55

Figure 3 represents the Pareto solutions graphically; it shows that for a specific number of channels correspond a specific stack height, a specific stack position and a specific spacing between plates. There is not only a single optimal solution that optimize the geometry of the regenerator and highlight the fact that the geometrical parameters are interdependent, which support the use of a multiobjective approach for optimization.

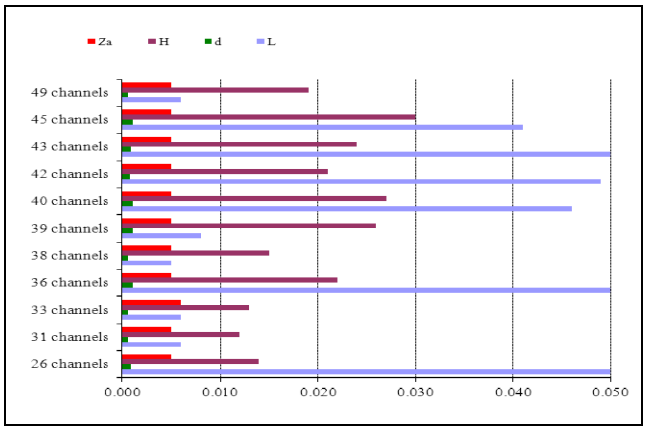

Fig.3. Optimal structural variables

These optimal solutions are then used to construct Figure 4 and Figure 5 representing respectively acoustic work, viscous resistance, conductive, convective and radiative heat fluxes obtained for different values of N. For maximum performance of the device, the acoustic power has to be maximized and the viscous resistance and thermal losses minimized. The conflicting nature of the five objectives can be observed in those profiles. For instance, while the acoustic power, the viscous resistance, the convective and the radiative heat fluxes decrease between 26 and 31 channels, the conductive heat flux increases (with L*, d*, H* and Za* given respectively in Table III).

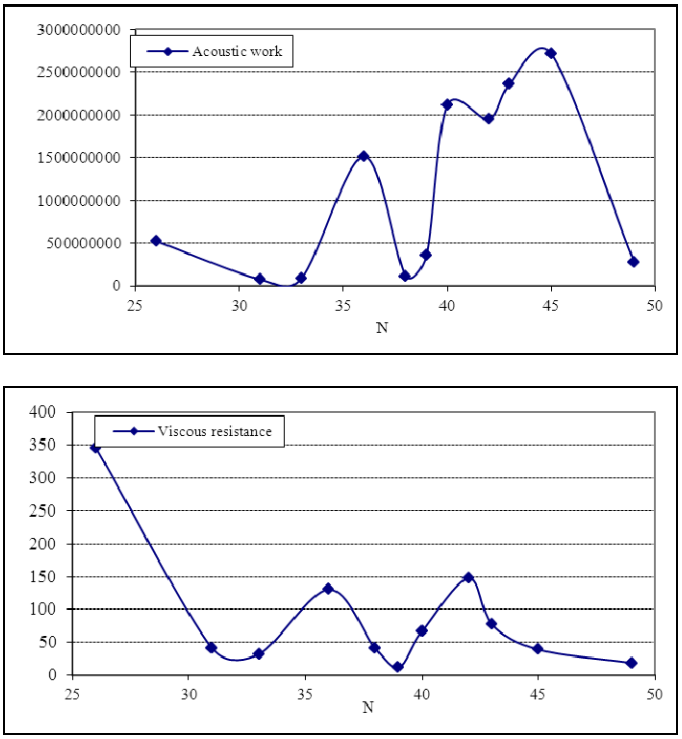

Fig.4. Acoustic power, viscous resistance plotted as a function of N

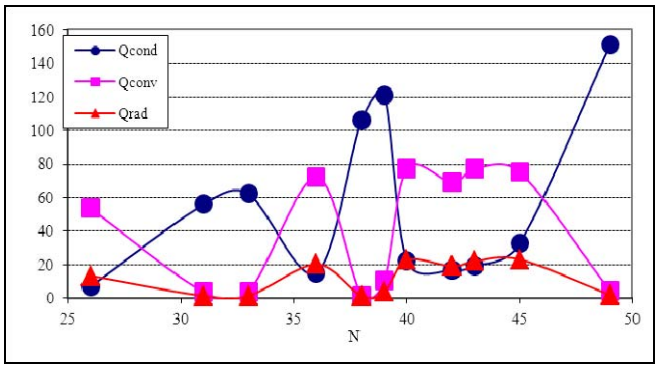

Fig.5. Conductive, convective and radiative heat fluxes plotted as a function of N

V. CONCLUSION

In order for a thermoacoustic engines to be competitive on the current market, they have to be optimized in order to improve its overall performance. Previous studies have relied heavily upon parametric studies. This work target the geometry of the thermoacoustic regenerator and uses multiobjective optimization approach to find the optimal set of geometrical parameters that optimizes the device. Five different objectives have been identified; a weight has been given to each of them to allow the designer to place desired emphasis. Mixed-integer nonlinear programming for thermoacoustic regenerator has been implemented in Gams. For the cases of multiobjective optimization, a nonlinear programming for thermoacoustic regenerator has been implemented in Gams. We have applied an improved version of a well-known multiobjective solution method, i.e., the epsilon constraint method called augmented epsilon constraint method (AUGMENCON). The results found shows the interdependence between the geometrical parameters of the regenerator which support the use of our multiobjective approach to optimize the geometry of thermoacoustic engine. Although the efficient solutions of proposed model could be found using AUGMENCON method by using commercial optimization solver LINDOGLOBAL, it should be noted that the corresponding computational time grows exponentially with problem size. Therefore, developing heuristic or metaheuristic solution methods could be of great interest.

ACKNOWLEDGMENT

This research was supported by the Department of mechanical engineering at the Cape Peninsula University of Technology, Cape Town, South Africa.

REFERENCES

[1] Yuan, S.W.K. & Jung, H.H. 1999, "Thermal management of computer systems using active cooling of Pulse Tube refrigerators", American Society of Mechanical Engineers, EEP, pp. 2.

[2] Joshi, Y.K. & Garimella, S.V. 2003, "Thermal challenges in next generation electronic systems", Microelectronics Journal, vol. 34, no. 3, pp. 169.

[3] Abdel-Rahman, E., Azenui, N.C., Korovyanko, I. & Symko, O.G. 2002, "Size considerations in interfacing thermoacoustic coolers with electronics", Thermomechanical Phenomena in Electronic Systems - Proceedings of the Intersociety Conference, pp. 421.

[4] Garrett, S. L., Hofler, T.J., Perkins, D.K. "Thermoacoustic refrigeration". Refrigeration and air conditioning technology workshop. June 23-25, 1993.

[5] Swift G.W. 1988. "Thermoacoustic engines". J Acoust Soc Am, vol. 4, pp.1146–80.

[6] Wheatley J.C, Hofler T, Swift G.W, Migliori A. 1985. "Understanding some simple phenomena in thermoacoustics with applications to acoustical heat engines". Am J Phys, vol. 53, pp.147–62.

[7] Garrett, S. and Hofler, T. Thermoacoustic Refrigeration, Technology 2001. NASA Conference Publication 3136, vol. 2, 1991, p. 397.

[8] Swift, G.W. 1995, "Thermo acoustic engines and refrigerators", Physics Today, vol. 48, no. 7, pp. 22-28.

[9] Minner, B.L., Braun, J.E. & Mongeau, L.G. 1997, "Theoretical evaluation of the optimal performance of a thermoacoustic refrigerator", ASHRAE Transactions, pp. 873.

[10] Wetzel, M. & Herman, C. 1997, "Design optimization of thermoacoustic refrigerators", International Journal of Refrigeration, vol. 20, no. 1, pp. 3-21.

[11] Besnoin, E. Numerical study of thermoacoustic heat exchangers, Ph.D. thesis, Johns Hopkins University (2001).

[12] Tijani, M.E.H., Zeegers, J.C.H. & De Waele, A.T.A.M. 2002, "The optimal stack spacing for thermoacoustic refrigeration", Journal of the Acoustical Society of America, vol. 112, no. 1, pp. 128-133.

[13] Zink, F., Waterer, H., Archer, R. & Schaefer, L. 2009, "Geometric optimization of a thermoacoustic regenerator", International Journal of Thermal Sciences, vol. 48, no. 12, pp. 2309-2322.

[14] Trapp, A.C., Zink, F., Prokopyev, O.A., Schaefer, L. 2011. "Thermoacoustic heat engine modeling and design optimization". Journal of Applied Thermal Engineering, vol. 31, pp. 2518-2528.

[15] Generalized Algebraic modelling Systems, (GAMS), [online] available: http://www.gams.com.

[16] Swift, G.W, Thermoacoustics: a unifying perspective for some engines and refrigerators. Acoustical society of America, Melville NY, 2002.

[17] Hwang, C.L., Masud, A. 1979. Multiple Objective Decision Making. Methods and Applications: A state of the art survey. Lecture Notes in Economics and Mathematical Systems Vol. 164. Springer-Verlag, Berlin.

[18] The MathWorks, Inc., MATLAB User's Guide. The Math Works, Inc., 2007.

[19] Baehr, H.D., Stephan, K. Wärme - und Stoffübertragung. (transl: Heat and Mass Transfer), fourth ed. Springer, Heidelberg, 2004.

[20] Atchley, A.A. Hofler, T., Muzzerall, M.L., Kite, Chianing A.O. 1990. "Acoustically generated temperature gradients in short plates". Journal of Acoustical Society of America, vol. 88, pp. 251.

[21] Mavrotas, G., 2009. Effective implementation of the ε-constraint method in multiobjective mathematical programming problems. Ap. Math. Comp. 213, 455-465.

[22] Aghaei, J., Amjady, N., Shayanfar, H.A. 2009. Multi-objective electricity market clearing considering dynamic security by lexicographic optimization and augmented epsilon constraint method". Appl. Soft. Comp., vol. 11, no. 4, pp. 3846-3858.